Orderly Arranged NLO Materials Based on Chromophore-Containing Dendrons on Exfoliated Layered Templates

Yung-Chung Chen,[†] Tzong-Yuan Juang,[*,‡] Tzong-Ming Wu,[§] Shenghong A. Dai,[†] Wen-Jang Kuo,[||] Ying-Ling Liu,[⊥] Franklin M. C. Chen,[#] and Ru-Jong Jeng[*,†]

Department of Chemical Engineering, National Chung Hsing University, Taichung 402, Taiwan, Department of Applied Chemistry, National Chiayi University, Chiayi 600, Taiwan, Department of Materials Science and Engineering, National Chung Hsing University, Taichung 402, Taiwan, Department of Applied Chemistry, National University of Kaohsiung, Kaohsiung 811, Taiwan, Department of Chemical Engineering and R&D Center for Membrane Technology, Chung Yuan Christian University, Taoyuan 320, Taiwan, and Department of Natural and Applied Sciences (Chemistry), University of Wisconsin-Green Bay, Green Bay, Wisconsin 54311

ABSTRACT Three chromophore-containing dendrons were intercalated into montmorillonite layered silicates via an ion-exchange process. Enlarged *d* spacings ranging from 50 to 126 Å were achieved for these novel organoclays. After the organoclays were blended with a polyimide, the steric bulkiness of the dendrons and the interaction between dendron and polyimide resulted in an ordered morphology. The orderly arranged nanocomposites were characterized by a UV−visible spectrophotometer, a variable-temperature infrared spectrometer, and electro-optical modulation. The dendrons in layered silicates were capable of undergoing a critical conformational change into an ordered structure, indicated by the drastic changes of interlayer distances at certain packing densities. Electro-optical coefficients increased sharply from 0 to 6 pm/V while the conformational change occurred. Furthermore, the addition of a polyimide capable of interaction-induced orientation was found to exert an enhancing effect on the degree of the noncentrosymmetric alignment.

KEYWORDS: cationic exchange capacity • dendron • montmorillonite • order arrangement

INTRODUCTION

Organic nonlinear optical (NLO) materials have been widely reported in the past two decades because of their applications, such as optical waveguides, modulators to transfer data into optical waves, low-power wavelength conversion and tuning, and optical switching (1−5). Typically, second-order NLO properties are present in the polymers when the NLO chromophores are aligned in a noncentrosymmetric manner by a poling technique (3−7). In order to preserve the NLO properties, the randomization of the poled (aligned) NLO molecules has to be prevented by all means. Therefore, various strategies have been devised to achieve polar order without resorting to electric poling, which include Langmuir−Blodgett (LB) growth, molecular self-assembly, etc. (8−11).

Recently, layered inorganic compounds such as montmorillonite (MMT) have been widely used because of their excellent thermal and mechanical properties (12). In addition, ordered assembly behaviors have been investigated on the layered silicates. Lin et al. (13−15) first utilized amphiphilic molecules as intercalating agents to prepare a new breed of self-assembly nanocomposites. Moreover, Beall et al. (16) have explained the self-assembly of organic molecules on MMT plates which appears to be controlled by two factors—the anchoring role of the polar head groups and the hydrophobicity of peripheral groups. Apart from that, the molecular chains can be arranged in different conformations as different cationic exchange capacity (CEC) equivalents are incorporated between layered silicates (17, 18). Lin et al. (17) further utilized poly(oxypropylene)diamine as the intercalated agent to investigate how the CEC equivalents affect the conformation change between the layered silicates. In addition, Osman et al. (18) investigated this type of self-assembly while varying temperatures and CEC equivalents. As part of this endeavor, a new way for controlling the dendron conformations in layered silicate confinement via the intercalation of polyurea/malonamide dendrons with peripheral phenyl groups has been reported by us (19). Different CEC equivalents would play an important role in controlling the dendron conformations in layered silicate confinement.

Dendritic structure containing NLO polymers with site isolation effects that could achieve large electro-optical (EO) coefficients have been of great interest recently (20−25).

* To whom correspondence should be addressed. Tel:+886-4-22852581. Fax: +886-4-22854734. E-mail: rjjeng@dragon.nchu.edu.tw.
Received for review July 27, 2009 and accepted October 4, 2009
[†] Department of Chemical Engineering, National Chung Hsing University.
[‡] National Chiayi University.
[§] Department of Materials Science and Engineering, National Chung Hsing University.
[||] National University of Kaohsiung.
[⊥] Chung Yuan Christian University.
[#] University of Wisconsin-Green Bay.
DOI: 10.1021/am900499s

Scheme 1. Chemical Structures for DO3, Chromophore-Containing Dendrons (G1, G2, and G3), and Their Intercalated Conformations

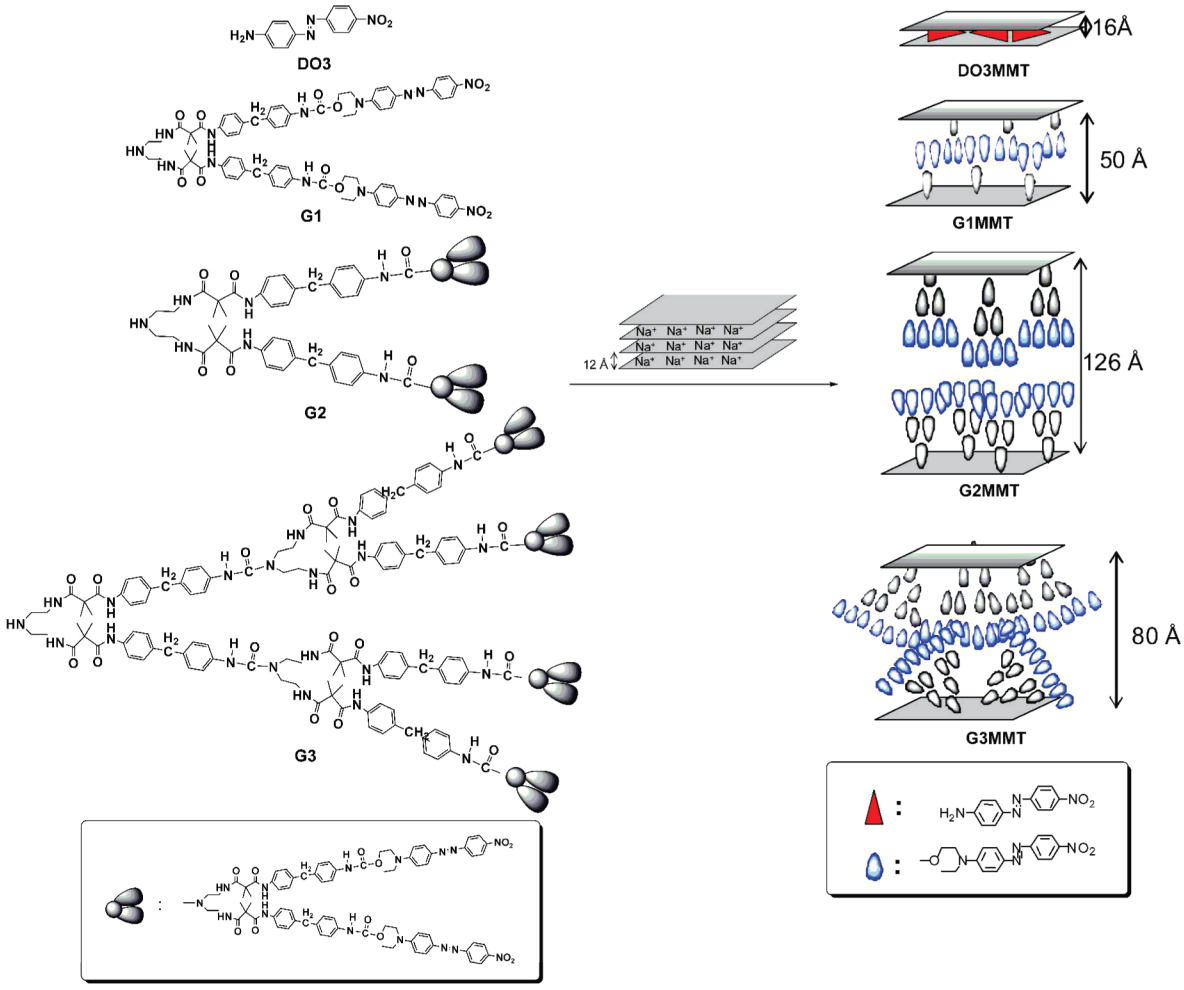

Because of their unique molecular sizes, shapes, and natures, dendritic structures can be precisely tailored with potential applications in self-assembly systems (26−28) and EO materials (20−25, 29).

In our preliminary study (30), dendrons with azobenzene dye (disperse red 1, DR1) in the exterior (G1, M_w = 1372; G2, M_w = 3488) (Scheme 1) were respectively utilized to form the amine salt, and these then proceeded to ion exchange with Na^+-MMT at equimolar CEC equivalents. After the dendron-modified organoclay was blended with a polyimide, the specific steric bulkiness of the dendrons and the interaction between layered silicates and indium tin oxide (ITO) glass substrates brought about a self-assembly arrangement that exhibited NLO properties without applying the poling process. Moreover, the usage of the host polyimide not only improved film formability but also provided interaction-induced orientation toward dendrons (31, 32). This idea was based on the $\pi-\pi$ stacking of polyimides that are widely used for liquid crystal (LC) alignment in LC displays (33−37). Moreover, Liu et al. (38) used a monocomponent polyimide bearing terminal hydrogen-bonding sites to form a unique spontaneous self-assembly behavior. It is concluded that the synergistic effect of $\pi-\pi$ stacking, dipolar interaction, and hydrogen bonding led to the self-assembled structures.

In this study, we further investigate the intercalating behavior of different generations of dendrons up to the dendron of generation 3 (G3, M_w = 7721) (Scheme 1). Additionally, we locate the critical concentration at which the conformational change will occur with the incorporation of different CEC equivalents onto the layered silicates (19). The dendron molecules would first be randomly distributed in the confined volume until reaching a critical concentration point. This conformational change would lead to noncentrosymmetric alignment of NLO chromophores: i.e., realization of NLO properties. Furthermore, we study the effect of a polyimide capable of interaction-induced orientation on the degree of the noncentrosymmetric alignment.

EXPERIMENTAL SECTION

Materials. Na^+-MMT, supplied by the Nanocor Co., is a sodium type with a cationic exchange capacity (CEC) of 1.20 mequiv g^{-1} and a surface area of 750 m^2 g^{-1}. Chromophore-containing dendritic structures (G1, G2 and G3; Scheme 1) were prepared via convergent routes in the same manner as reported by our laboratory (20, 30, 39−42). The molecular weights of intercalating agents are as follows: disperse orange 3 (DO3; Scheme 1), M_w = 242; G1, M_w = 1372; G2, M_w = 3488; G3, M_w

= 7721. Solvents used are as follows: tetrahydrofuran (THF, Tedia), distilled under nitrogen from sodium/benzophenone; toluene (Tedia), *N*,*N*-dimethylformamide (DMF, Tedia), and *N*,*N*-dimethylacetamide (DMAc, Tedia), were purified by distillation under reduced pressure over calcium hydride and stored over 4 Å molecular sieves.

Measurements. Differential scanning calorimetry (DSC) was performed by a Seiko SSC-5200 instrument at a heating rate of 10 or 20 °C/min under a nitrogen atmosphere. Thermogravimetric analysis (TGA) was carried out at a heating rate of 10 °C/min under an air atmosphere. X-ray diffraction (XRD) analysis was performed by using a 3 kW Rigaku III diffractometer with Cu target ($\lambda = 1.542$ Å), using a scanning rate of 2°/min. The d spacing of the intercalated MMT was analyzed by Bragg's equation ($n\lambda = 2d \sin \theta$). Transmission electronic microscopy (TEM) was performed with a Zeiss EM 902A instrument operated at 80 kV, and samples of approximately 70 nm thickness were microtomed at room temperature. UV−vis spectra were recorded on a Perkin-Elmer Lambda 2S spectrophotometer. Variable-temperature infrared spectrometer (VTIR) measurements were performed on a Perkin-Elmer Spectrum One Fourier transform infrared (FTIR) spectrometer at a heating rate of 10 °C/min from room temperature to 160 °C. A thin layer of silver was sputtered onto the films as a top electrode for EO measurement by a simple reflection technique (43).

Preparation of Organoclays with Equimolar CEC Equivalent (DO3MMT, G1MMT, G2MMT and G3MMT; Scheme 1) (30). G1MMT, G2MMT, and G3MMT were prepared according to a method described in the literature (30). Experimental procedures for preparing G3MMT in equimolar CEC equivalent are described as followx. First, Na^+-MMT (200 mg) was placed in a 100 mL beaker and dispersed into 20 mL of deionized water at 80 °C until fully swollen. For the G3 solution, the formulation was prepared by adding 1853 mg of the G3 sample to *N*,*N*-dimethylformamide (DMF), followed by acidifying the secondary aliphatic amines of G3 using hydrochloric acid (37% in water, 24 mg, 0.24 mmol). Subsequently, the amine salt solution was added to the swollen Na^+-MMT slurry. Finally, the suspension was stirred for 24 h at 80 °C. The resulting agglomerated precipitate was collected and then washed with water and DMF twice to thoroughly remove any residual ions and nonexchanged G3 dendron samples. The G3MMT was dried in a vacuum oven at 80 °C for 24 h and characterized by using XRD, TEM, TGA, and DSC. For comparison, an amine-containing azobenzene chromophore, disperse orange 3 (DO3, Scheme 1), was also utilized to prepare DO3MMT (Scheme 1).

Preparation of Nanocomposite Thin Films Comprised of Polyimide and Equimolar CEC Equivalent Organoclays (30). Polyimide was respectively mixed with 5 wt % of DO3MMT, G1MMT, G2MMT, and G3MMT in *N*,*N*-dimethylacetamide (DMAc) to constitute four guest−host nanocomposites: PI-DO3MMT, PI-G1MMT, PI-G2MMT, and PI-G3MMT (note: PI is the abbreviation for polyimide). The solutions were then cast onto the ITO glass substrates. The resulting films were dried at 60 °C in a vacuum oven overnight to ensure complete removal of any residual solvent.

Preparation of Organoclays with Different CEC Equivalents and Their Nanocomposite Thin Films. To investigate the conformation change at different concentrations and the NLO properties, various stoichiometric amounts of dendron (G1, G2, and G3) intercalating agents were prepared as an example by the following procedures. As the G1 dendron, Na^+-MMT (200 mg) was first dispersed and swollen in deionized water. Various equivalents of G1 amine salt solutions (0.25 CEC, 82 mg; 0.5 CEC, 164 mg; 0.75 CEC, 247 mg; 1.5 CEC, 494 mg; 2.0 CEC, 659 mg) were respectively added to the slurry. The suspension was stirred for 24 h at 80 °C. The resulting agglomerated precipitate was collected and then washed with water and THF twice to thoroughly remove any residual ions and nonexchanged G1 dendron samples. Moreover, the organoclays of the G2 and G3 series were prepared in the same manner as the procedure described above.

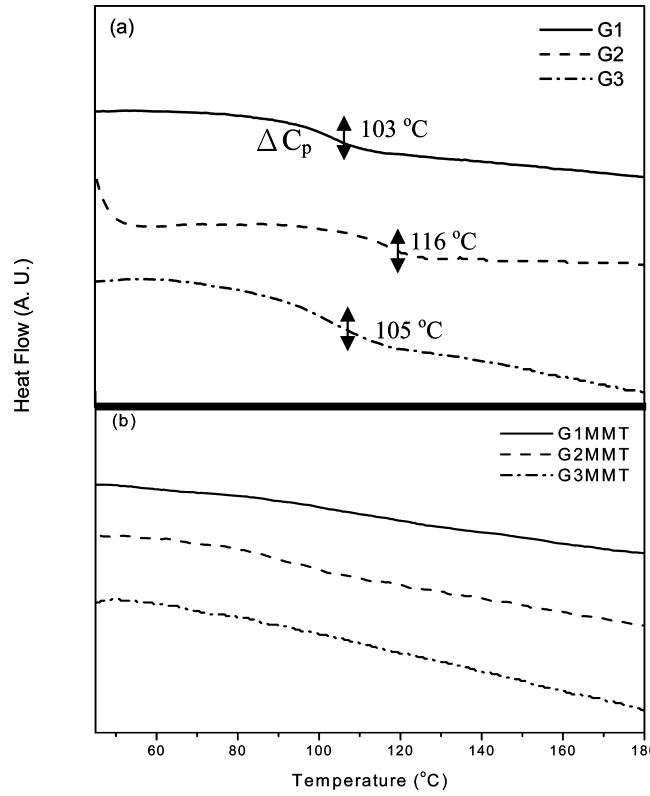

FIGURE 1. DSC thermograms for (a) pristine chromophore-containing dendrons G1, G2, and G3 and (b) dendron-containing organoclays G1MMT, G2MMT, and G3MMT.

A series of nanocomposites were prepared by mixing 5 wt % of the modified organoclays with different CEC ratios with the polyimide sample. Thin films were also prepared using solvent casting to investigate the packing density effect on the NLO properties.

RESULTS AND DISCUSSION

In this study, DO3 and three generations of dendrons (G1, G2, and G3) were used as the intercalation agents to modify the layered silicates. As shown in Scheme 1, four organoclays (DO3MMT, G1MMT, G2MMT, and G3MMT) were prepared according to the procedures described in the literature (30). The modified organoclays were characterized by DSC, TGA, XRD, and TEM. Figure 1 shows DSC thermograms of these dendrons (G1, G2, and G3) attached to the layered silicates. The G1, G2, and G3 dendrons exhibited T_g's at 103, 116, and 105 °C, respectively. These T_g's almost disappeared after modification. This implies that the dendrons between the layered silicates were restricted without sufficient spaces for molecular relaxation. This observation is in agreement with those reported in the literature (19, 41). Moreover, the TGA study indicates that the actual organic/inorganic ratios (W_O/W_I) of 24/76 for DO3MMT, 64/36 for G1MMT, 80/20 for G2MMT, and 82/18 for G3MMT are consistent with the theoretical organic fractions based on the originally intended CEC ratios (Table 1). For example, for

Table 1. Organic/Inorganic Fractions, *d* Spacings and Dispersibility of the Modified Organoclays

		weight ratio (% w/w)		dispersibility[d]			
intercalation agent	*d* spacing (Å)[a]	based on CEC[b]	based on TGA[c]	H_2O	THF	toluene	DMAc
DO3MMT	16	19/81	24/76	−	−	−	+
G1MMT	50	62/38	64/36	−	+−	−	+−
G2MMT	126	80/20	80/20	−	+−	−	+
G3MMT	80	90/10	82/18	−	+−	−	+

[a] Silicate-layer thickness determined by XRD patterns for DO3MMT and G1MMT and TEM images for G2MMT and G3MMT. [b] Values calculated from the following equation: $X(1.2 \times 10^{-3})M_w = Y$, where X is the pristine weight of the clay, M_w is the molecular weight of the dendron, and Y is the weight of the dendron. The theoretical organic ratio is given by $Y/(X + Y)$. [c] Measured by thermogravimetric analysis (TGA) in air. [d] Legend: +, dispersible; +−, aggregate after 12 h; −, aggregate.

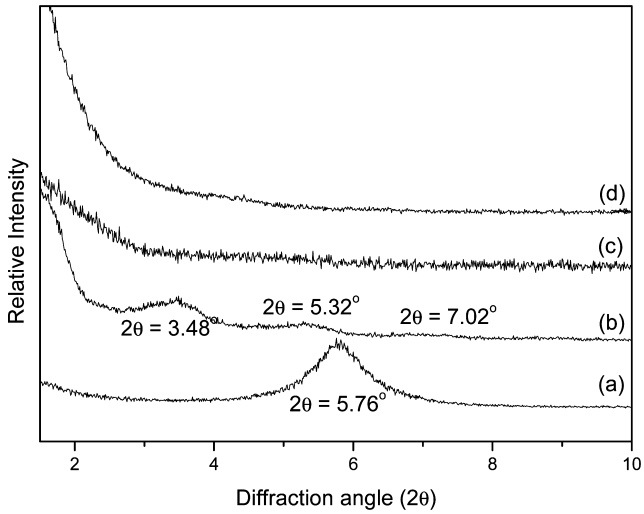

FIGURE 2. XRD diffraction patterns of the modified organoclay: (a) DO3MMT; (b) G1MMT; (c) G2MMT; (d) G3MMT.

G1MMT at 1.0 CEC equivalent, a theoretical organic/inorganic ratio of 62/38 is derived, which is close to the number (64/36) obtained from the TGA study. Hence, it is evident that all the aforementioned chromophore-containing dendrons are capable of intercalating the layered silicates. Furthermore, the dispersibility of these modified organoclays is also given in Table 1. These organoclays could be well dispersed in DMAc without precipitation or aggregation after a long period of time. Therefore, a series of organic/inorganic nanocomposites were prepared using DMAc as medium.

The morphology of these organoclays was obtained via XRD and TEM microscopic investigation, and their *d* spacings are summarized in Table 1. Figure 2 shows the X-ray diffraction patterns of modified organoclays (DO3MMT, G1MMT, G2MMT, and G3MMT) at equimolar CEC equivalents. In the spectra, the *d* spacings of DO3MMT and G1MMT based on Bragg's law ($n\lambda = 2d \sin\theta$ and the observed values for $n = 2, 3, 4$, etc.) were 16 and 50 Å, respectively. However, no diffraction peaks were found for the G2MMT and G3MMT samples. This means the *d* spacings of layered silicate are greater than 58 Å. In order to confirm the results

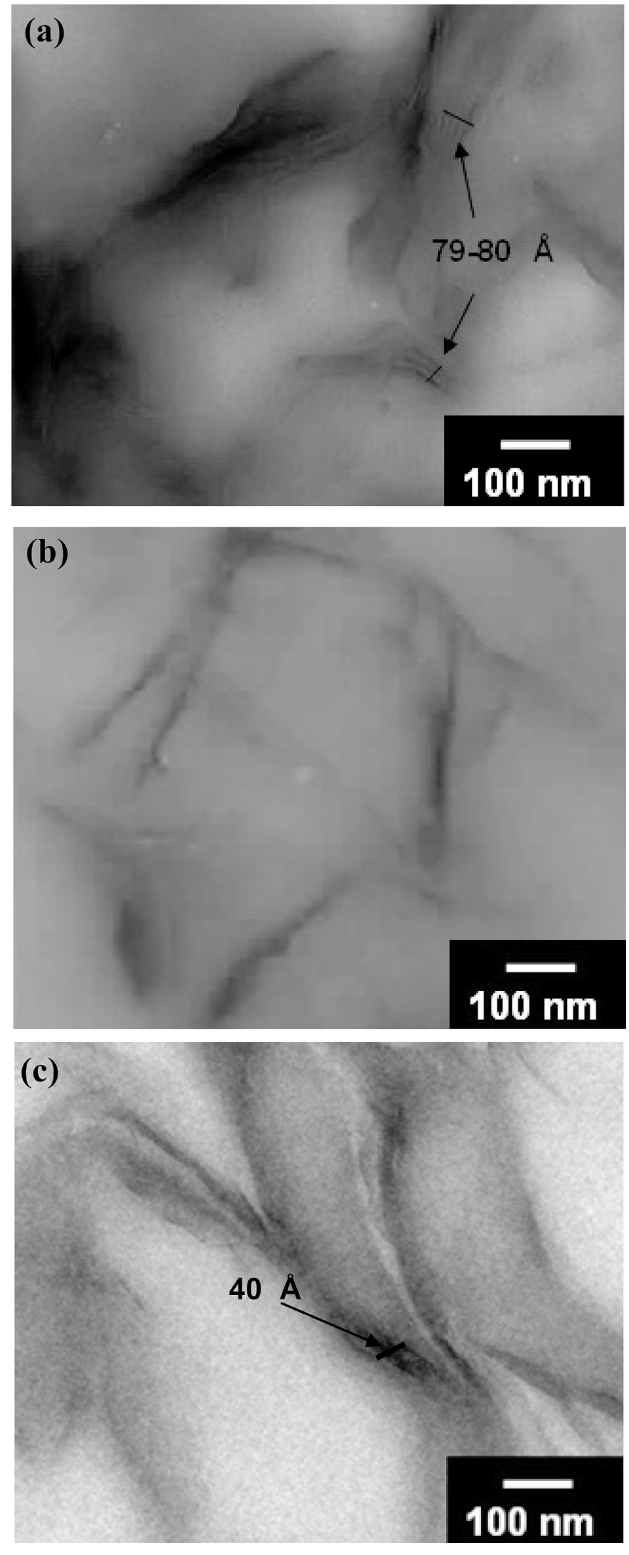

FIGURE 3. TEM microscopic images: (a) intercalated morphology of G3MMT (100 nm); (b) exfoliated morphology of PI-G3MMT (100 nm); (c) intercalated morphology of PI-DO3MMT (100 nm).

of the XRD study, TEM was utilized to visualize the spatial distribution for G2MMT and G3MMT. The TEM micrograph of G2MMT (30) exhibited intercalated *d* spacings larger than 120 Å. However, the TEM micrograph of G3MMT revealed intercalated behavior, and the *d* spacing was smaller than that of G2MMT (Figure 3a). This might be due to the larger

Table 2. NLO Properties for PI-Organoclay Nanocomposites

sample	T_g (°C) [a]	dye content (%)	r_{33} (pm/V)[b]
PI-DO3MMT	ND	5.0	0
PI-G1MMT	ND	2.3	5.7
PI-G2MMT	ND	1.8	5.1
PI-G3MMT	ND	1.6	4.1

[a] Data taken from DSC second heating traces, with a heating rate of 20 °C/min at nitrogen. [b] EO coefficient without applying poling process which was measured at 830 nm.

molecular size of G3, which is not capable of intercalating into the layered silicates completely (44). A conceptual representation of the intercalation conformations for the organoclays is shown in Scheme 1. From the pervious study (30), the PI-G1MMT and PI-G2MMT samples exhibited exfoliated morphology, determined by XRD and TEM micrographs. As for the PI-G3MMT nanocomposite in this study, no diffraction peak was observed at $2\theta = 1.5-10°$, which also means the *d* spacing within the layered silicate was at least larger than 58 Å. In addition, the PI-G3MMT sample whose TEM micrograph is shown in Figure 3b also exhibited exfoliated morphology. On the basis of the results shown above, all the nanocomposites containing dendrons exhibited exfoliated morphology due to sufficiently large interlayered *d* spacings of modified organoclays. Therefore, the polymer chains would be able to enter the layered silicates and subsequently to form the exfoliated morphology. In contrast, the TEM micrograph of the PI-DO3MMT sample shown in Figure 3c indicates that intercalation morphology (40 Å) was present throughout the nanocomposite. This is because a much narrower *d* spacing (16 Å) was obtained for the pristine DO3MMT organoclay. Therefore, most of the polyimide chains were not able to intercalate the clay galleries.

After solvent-casting these four nanocomposites (PI-DO3MMT, PI-G1MMT, PI-G2MMT, and PI-G3MMT) onto the ITO glass substrates, respectively, a simple reflection technique was utilized to measure the EO coefficients of these dried thin films (Table 2) (43). According to the literature (30), the pristine PI-G1MMT and PI-G2MMT samples were capable of exhibiting EO coefficients due to the ordered alignment between the dendron structure and MMT, which would make the dendron fixated on the layered silicate platelets in the same direction. Moreover, the presence of polyimide did not interfere with the degree of ordered alignment. In this study, the pristine PI-G3MMT sample exhibited an r_{33} value of 4.1 pm/V. It is important to note that the chromophore content for PI-G3MMT (1.6%) is quite low, yet a reasonable EO coefficient was achieved. This implies that an ordered arrangement of NLO chromophores was also present in this pristine nanocomposite sample. In addition, the polyimide might have an interaction-induced orientation effect on the ordered arrangement (32, 33). On the other hand, optical nonlinearity was not observed for the pristine PI-DO3MMT sample due to the presence of intercalated morphology (Figure 3c). This indicates that the

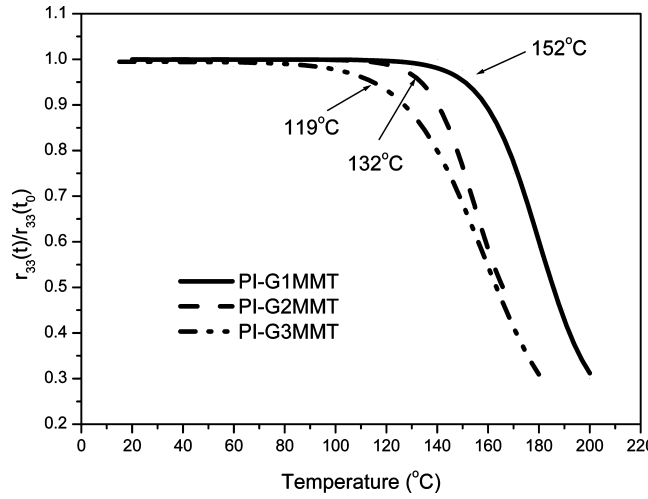

FIGURE 4. Thermal dynamic properties of PI-G1MMT, PI-G2MMT, and PI-G3MMT.

exfoliated layered structures and steric bulkiness of the dendrons play critical roles in achieving ordered morphology.

In general, the EO coefficient of NLO polymers remains stable at low temperatures but decays significantly at a specific temperature. This specific temperature is defined as the effective relaxation temperature (5, 20). This value provides invaluable information on the randomization of ordered arrangement, i.e. aligned chromophores, and allows one to be able to evaluate the transition stage between ordered and disordered morphology. To assess the ordered arrangement, the effective relaxation temperature was utilized to determine the orientation of the dendron molecules and to further comprehend the ordered arrangement (30). Figure 4 shows dynamic thermal stability of the pristine samples. The effective relaxation temperatures for the PI-G1MMT, PI-G2MMT, and PI-G3MMT samples are at 152, 132, and 119 °C, respectively. These results indicate that drastic conformational change would occur at this one particular temperature. Therefore, the UV−vis spectrophotometer was utilized after 1 h thermal treatment at 140, 120, and 110 °C for PI-G1MMT, PI-G2MMT, and PI-G3MMT, respectively, to investigate the ordered arrangement. In UV−vis spectra (Figure 5), the absorption maxima of these three nanocomposite thin films blue-shifted and decreased to certain levels after the thermal treatments. This phenomenon might be due to the self-association of the bulky dendrons to form intramolecular H-type aggregates, which is detrimental to NLO properties (45). Due to the self-assembly nature, the original ordered arrangement is more stable than the H-type aggregates. Therefore, the H-type aggregates would relax to the approximately original conformation after cooling down to 100 °C for a certain period of time. However, the H-type aggregates could not recover fully to the original conformation while cooling down to room temperature, even after a long time period of time (30). In this study, we also investigated the influence of the dendron generations (Figure 5). The PI-G3MMT sample with the larger size dendron G3 recuperated more quickly to the original conformation. This might be due to the fact that the cooling temperature

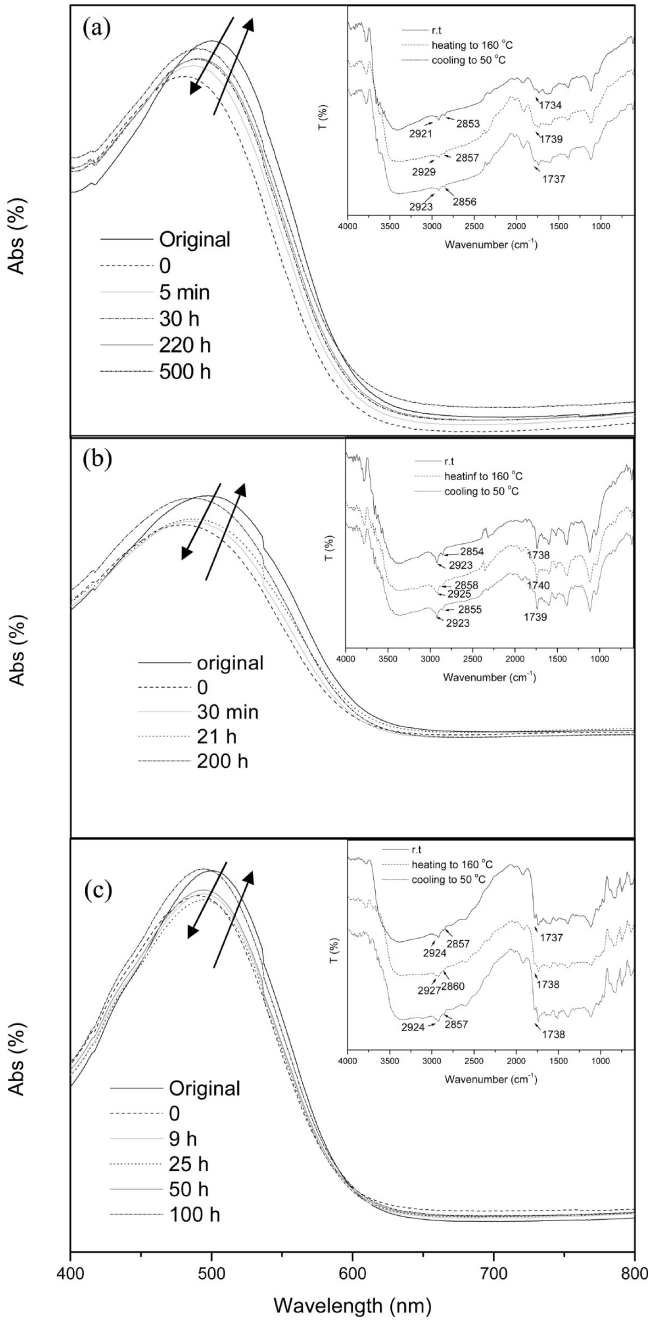

FIGURE 5. UV−vis spectra for molecular motion behavior: (a) PI-G1MMT for thermal treatment at 140 °C for 1 h and cooling to 100 °C and (inset) the VTIR spectra for PI-G1MMT; (b) PI-G2MMT for thermal treatment at 120 °C for 1 h and cooling to 100 °C, and (inset) the VTIR spectra for PI-G2MMT; (c) PI-G3MMT for thermal treatment at 110 °C for 1 h and cooling to 100 °C and (inset) the VTIR spectra for PI-G3MMT.

(100 °C) was close to the relaxation temperature of PI-G3MMT (119 °C). Moreover, due to the larger size of G3, stronger van der Waals forces, $\pi-\pi$ interactions, and dipolar attractions between the G3 dendrons and polyimide would cause the dendrons to recover to their original conformation easily. In addition, the VTIR spectra of these nanocomposites are also presented in the insets of Figure 5. All three of these nanocomposites exhibited the characteristic absorption bands, which blue-shifted slightly after thermal treatment (46). As the temperature decreased, the absorption bands

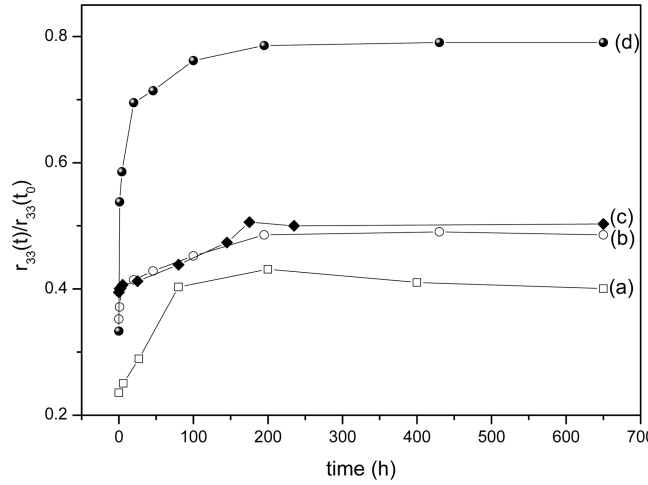

FIGURE 6. Temporal behavior of EO coefficients: (a) PI-G1MMT thermal treatment at 140 °C for 1 h and subsequent cooling to room temperature; (b) PI-G2MMT thermal treatment at 120 °C for 1 h and subsequent cooling to room temperature; (c) PI-G3MMT thermal treatment at 110 °C for 1 h and subsequent cooling to room temperature; (d) PI-G2MMT thermal treatment at 120 °C for 1 h and then annealing at 100 °C.

started to red-shift. This observation is consistent with the results of the UV−vis study.

As mentioned earlier, the thermal treatment influences the ordered arrangement of the NLO chromophores, since it induces the drastic conformational change. In addition, H-type aggregates would influence the ordered arrangement of NLO chromophores negatively. Therefore, the temporal behaviors of the EO coefficients for the PI-G1MMT, PI-G2MMT, and PI-G3MMT samples after 1 h thermal treatment at 140, 120, and 110 °C, respectively, were also studied. Parts a−c of Figure 6 show the EO coefficients for the thermal-treated PI-G1MMT, PI-G2MMT, and PI-G3MMT samples while remaining at room temperature. After the thermal treatment, the r_{33} values of these three samples retained about 30% of their original values. As the thermal-treated samples cooled from 140, 120, and 110 °C, respectively, to room temperature, the r_{33} values started to increase in an extremely slow manner. They only reached approximately 40−50% of their original values for a long period of time (650 h). The PI-G3MMT sample with the larger size of dendron G3 recuperated more quickly to the original conformation. Moreover, the r_{33} value started to increase in a relatively faster manner when the annealing temperature was 100 °C for the PI-G2MMT sample (cooled from 120 °C) (Figure 6d). Its r_{33} value could reach approximately 80% of its original value after 200 h. This is consistent with the UV−vis investigation. On the basis of the above observation, the annealing temperature does play a critical role in reversing back to the original self-organized structures. To some extent, it appears that the closer the annealing temperature to the effective relaxation temperature, the greater the extent of NLO recovery ratios they attain.

The PI-G1MMT, PI-G2MMT, and PI-G3MMT nanocomposites mentioned above were in 1.0 CEC equivalents. However, according to the previous literature (17−19), surface modifications using different CEC equivalents led to various

Table 3. Intercalation Profiles of Organoclays with Various CEC Equivalents

dendron/CEC of clay molar ratio	*d* spacing (Å)[a]	weight ratio (% w/w) based on CEC[a]	weight ratio (% w/w) based on TGA[c]	dispersibility[d] H_2O	dispersibility[d] THF	dispersibility[d] DMAc
		Chromophore G1				
0.25	15	29/71	36/64	+−	+−	+−
0.5	28	45/55	49/51	+−	+−	+−
0.75	35	55/45	58/42	−	+−	+−
1.0	50	62/38	64/36	−	+−	+−
1.5	53	71/29	74/26	−	+−	+
2.0	53	77/23	79/21	−	+−	+
		Chromophore G2				
0.25	15	51/49	57/43	−	+−	+−
0.5	57	68/32	69/31	−	+−	+
0.75	62	76/24	81/19	−	+−	+
1.0	126[e]	80/20	80/20	−	+−	+
1.25	130−140 /exfoliation[e]	84/16	87/13	−	+−	+
1.5	exfoliation[e]	86/14	86/14	−	+−	+
		Chromophore G3				
0.25	15	70/30	72/28	−	+−	+−
0.5	15	82/18	82/18	−	+−	+
0.75	37	87/13	87/13	−	+−	+
1.0	80[e]	90/10	82/18	−	+−	+
1.25	exfoliation[e]	92/8	94/6	−	+−	+
1.5	exfoliation[e]	93/7	93/7	−	+−	+

[a] Silicate-layer thickness determined on XRD pattern. [b] Values calculated from the following equation: $X(1.2 \times 10^{-3})M_w = Y$, where X is the pristine weight of clay, M_w is the molecular weight of the dendron, and Y is the weight of the dendron. The theoretical organic ratio is given by $Y/(X + Y)$. [c] Measured by thermogravimetric analysis (TGA) in air. [d] LegendL +, dispersible; +−, aggregate after 12 h; −, aggregate. [e] Determined by TEM microscopy.

particular conformations. Hence, the EO coefficients of the nanocomposites with different CEC equivalents might provide certain information to investigate the ordered arrangement behavior of these types of nanocomposites. Therefore, various molar ratios of dendron (G1, G2, and G3) modified MMT were prepared and their interlayer distances and conformation changes as well as NLO properties were also studied. The intercalated behavior and morphology studied by XRD patterns and TEM microscopy are summarized in Table 3. Figure 7 shows the XRD pattern of the G1/MMT organoclays. In G1 dendron/MMT organoclays, the *d* spacings were observed from 15 to 53 Å throughout the increased ratio of dendron/MMT up to 2 CEC equivalents. As the amount of G1 dendron increased from 0.25 to 1.0 CEC in the modified MMT samples, the *d* spacing of the layered silicates was increased from 15 to 50 Å. On further addition of the G1 molecule to the samples with 1.5 and 2.0 CEC equivalents, the *d* spacing remained unchanged at 53 Å for both samples, which was close to that of the sample with 1.0 CEC equivalent (50 Å). This is possibly due to the fact that the surface of MMT had been fully ion-exchanged and occupied by a G1 dendron with 1.0 CEC equivalent or higher. This observation is consistent with those reported in the literature (17, 19).

Moreover, the intercalation profiles of the *d* spacings for the modified MMT samples with the large molecular size dendrons (G2 and G3) were also obtained using the same procedures (Table 3). For G2 dendron/MMT organoclays, the

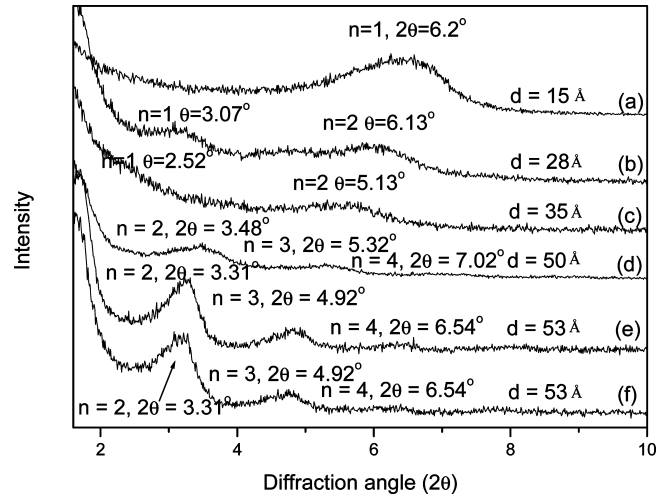

FIGURE 7. X-ray diffraction patterns of intercalation with various chromophore G1/CEC of clay molar ratios: (a) 0.25; (b) 0.50; (c) 0.75; (d) 1.0; (e) 1.5; (f) 2.0.

d spacing only reached 15 Å when the loading ratio was 0.25 CEC equivalent. This is because the number of dendrons is not large enough to resist the attraction between layered silicates. As the amount of G2 dendrons for intercalation increases (0.5−1.0 CEC), the space was further increased with the dendritic structures up to 126 Å. As the G2/MMT molar ratio increased from 1.0 to 1.5 CEC equivalents, no diffraction peak was observed, indicating that the *d* spacing of layered silicate was larger than 58 Å. This is because the

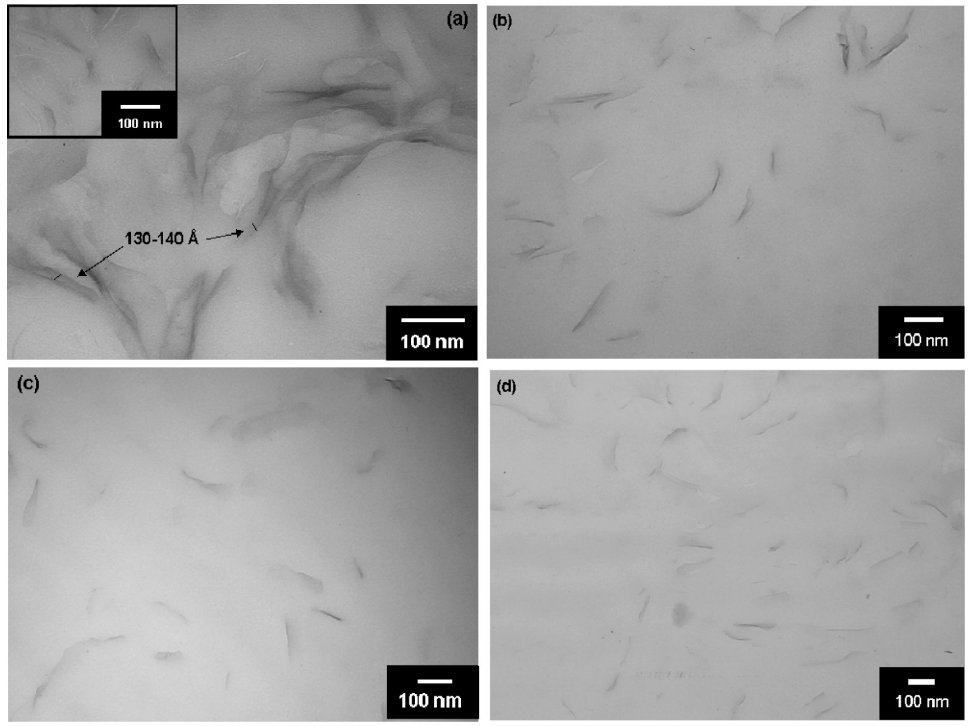

FIGURE 8. TEM microscopic images: (a) intercalated and exfoliated (inset) morphology of 1.25CEC-G2MMT (100 nm); (b) exfoliated morphology of 1.5CEC-G2MMT (100 nm); (c) exfoliated morphology of 1.25CEC-G3MMT (100 nm); (d) exfoliated morphology of 1.5CEC-G3MMT (100 nm).

G2 dendrons suddenly formed a perpendicular chain arrangement between the layered silicates to enlarge the *d* spacings. A similar observation was also reported in the literature (47). The conformational effects of CEC equivalents on the intercalated behaviors for the G3 dendron/MMT organoclays were also observed.

In order to confirm the XRD results, TEM was utilized to visualize the spatial distribution between the layered silicates. As the molar ratio was 1.25 CEC equivalent, the G2 dendron/MMT organoclay exhibited partially intercalated (Figure 8a) and exfoliated (Figure 8a inset) morphology. However, the G3 dendron/MMT organoclay (Figure 8b) exhibited fully exfoliated morphology at 1.25 CEC equivalent. The exfoliated morphology might be due to G3 molecules with a larger molecular size and stronger intermolecular interactions. In addition, as the CEC ratio was increased to 1.5 equivalent, both the G2 dendron/MMT (Figure 8c) and G3 dendron/MMT organoclays (Figure 8d)

Scheme 2. Conceptual Representation of Possible Conformations for Respective Intercalating MMTs with G1, G2, and G3 Dendrons

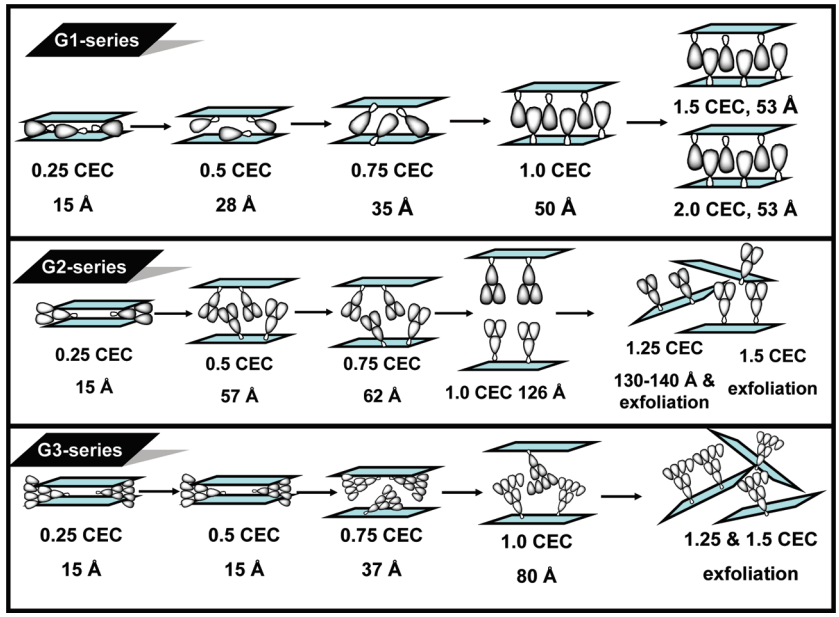

exhibited exfoliated morphology. The large number of dendrons and strong intermolecular interactions played critical roles, resulting in a fully extension of dendrons onto the layered silicates and forming the exfoliated behavior, which has never been reported in the literature. A possible conceptual model of the conformation change with respect to the relative concentrations in the gallery is proposed in Scheme 2. The intercalating phenomena can be clearly illustrated and are strongly dependent on the dendritic structures as well as the amount of the dendrons onto the layered silicates. Moreover, the DR1-terminated malonamide dendrons with strong dipole−dipole and hydrogen-bonding interactions also provide the possibility of self-association.

The char yields measured by TGA (Table 3) reveal that the amounts of incorporated dendrons are consistent with the theoretical calculations based on CEC. In order to fabricate the polymer thin films on the substrate, it is essential to acquire well-dispersed organoclays. Hence, the dispersibility of organoclays based on different CEC equivalents is presented in Table 3. For the G1MMT organoclays with different CEC equivalents, good dispersibility in hydrophilic solvent (H_2O) was observed when the molar ratio was lower than 0.5 CEC equivalent. As the molar ratio was larger than 0.5 CEC equivalent, the G1MMT samples exhibited good dispersibility in organic solvents. However, for the G2MMT and G3MMT organoclays with various CEC equivalents, good dispersibility in organic solvents such as THF and DMAc was observed, but all the samples aggregated in H_2O. This might be due to the presence of more hydrophobic segments in G2 and G3. Therefore, all the organoclays could disperse well in DMAc, along with the polyimide.

The *d* spacings of the various molar ratios derived from the three generations of dendrons (G1, G2, and G3) and the EO coefficients for the organoclays mixed with the polyimide are shown in Figure 9. For the PI-G1MMT series nanocomposites, optical nonlinearity was not observed for the samples containing organoclays with molar ratios lower than 0.5 CEC equivalent. This might be due to the fact that the dendrons preferred the tilting conformation at lower molar ratio, resulting in a random arrangement. In addition, the narrower *d* spacing of the modified organoclays also limited the possibility for the migration of polyimide chains into the clay galleries, leading to the intercalated morphology (inset of Figure 9). As the amount of G1 dendron increased in the range from 0.75 to 1.5 CEC in the nanocomposite samples, the EO coefficients increased with increasing molar ratio. In this case, the closely packed dendrons would develop into an extended morphology and eventually form a perpendicular conformation: i.e., noncentrosymmetric alignment. Moreover, an increase of the hydrogen-bonding interactions, dipolar attractions, and $\pi-\pi$ stacking might also play a part, resulting in ordered arrangement (12, 37, 48). However, as the amount of G1 dendron increased up to 2.0 CEC equivalent in the nanocomposite sample, the EO coefficient did not increase further. This indicates the degree of noncentrosymmetric alignment, i.e. ordered morphology, remained virtually the same for the samples comprising organoclays with higher CEC equivalents. Similar nonlinear optical behavior was also observed for PI-G2MMT and PI-G3MMT nanocomposites with various CEC equivalents. For a PI-G2MMT sample with 0.5 CEC equivalent, the r_{33} value was 2.5 pm/V. This is due to the presence of the larger *d* spacing of G2MMT layered silicates at 0.5 CEC equivalent. This large *d* spacing could easily provide the space for the polyimide chain to intercalate into the galleries, leading to formation of the exfoliated morphology. As mentioned earlier, the exfoliated morphology is the essential prerequisite for ordered arrangement. In addition, this critical CEC equivalent of the dendrons in organoclays provides a transitional conformation change to the ordered arrangement.

The G3 dendron, with the largest molecular weight, is capable of exhibiting film formability. G3MMTs (1.25 and

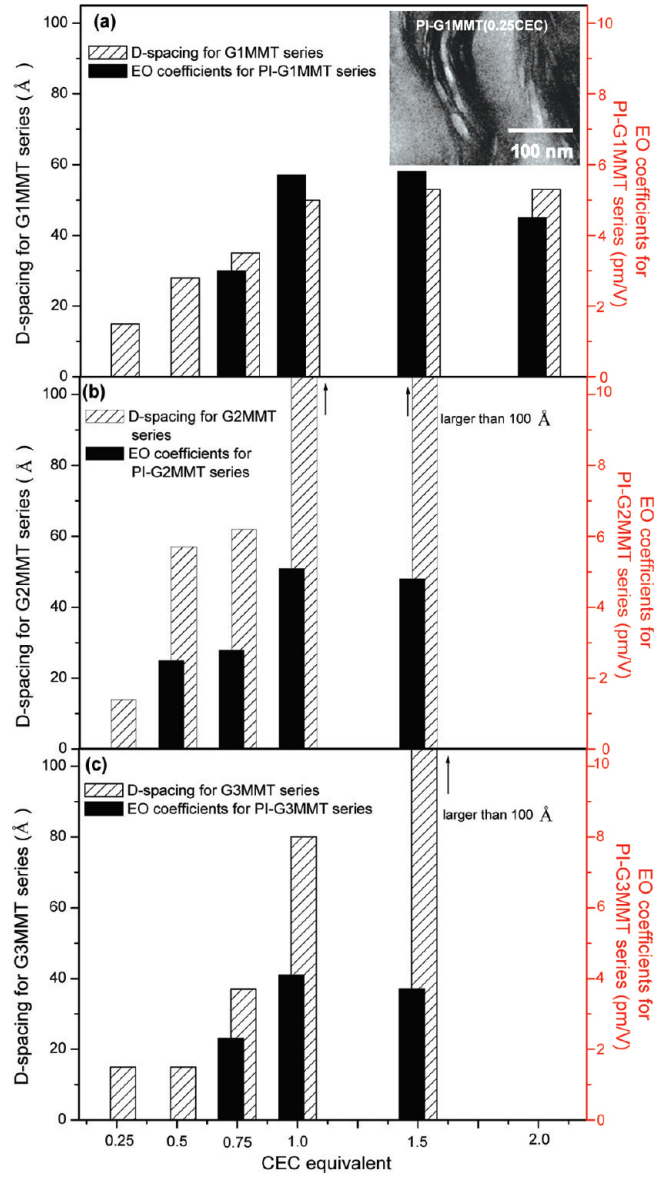

FIGURE 9. EO coefficients for the nanocomposites comprising organoclays with different CEC equivalents and *d* spacing profile for organoclays with different CEC equivalents: (a) G1 series; (b) G2 series; (c) G3 series. The inset is a TEM image of the PI-G1MMT (0.25CEC).

1.5 CEC) with exfoliated morphology were investigated for their optical nonlinearity. The pristine G3MMT (1.25 CEC) thin film exhibited an EO coefficient of 7.1 pm/V. Without the presence of polyimide, the intermolecular interactions would result in self-association among the dendrons (24, 36, 49). However, the association behavior resulted in a lower EO coefficient for the G3MMT (1.25 CEC) organoclay (dye content 30.1%). This is possibly because the nonionic-exchanged dendrons would interfere with ordered alignment of the dendrons upon the silicate platelets. Furthermore, the effective relaxation temperature was also measured to determine the orientation behavior. The effective relaxation temperature for the G3MMT (1.25 CEC) sample was 92 °C. The G3MMT (1.25 CEC) sample was thermally treated at 80 °C for 1 h to investigate the ordered arrangement in the same manner mentioned previously. As the thermal-treated sample was cooled from 80 °C to room temperature, the r_{33} value started to increase in an extremely slow manner. It only reached approximately 40% of its original value for a long period of time. In addition, as the thermal-treated sample was annealed at 70 °C, the r_{33} value started to increase in a relatively faster manner. This indicates that the G3MMT sample recuperated more quickly to the original ordered conformation at 70 °C. In addition, for the G3MMT sample with 1.5 CEC equivalent, the EO coefficient was 4.9 pm/V, which was smaller than that of G3MMT (1.25 CEC). The decrease of the EO coefficient further indicates that the presence of more nonionic-exchanged dendrons would interfere with the ordered alignment of dendrons upon the silicate platelets to a greater extent.

CONCLUSION

Using the chromophore-containing dendrons (G1, G2, and G3) as the intercalating agents allowed the preparation of highly ordered silicates with the interlayer *d* spacing up to 126 Å, which is 10 times the value for the pristine layered silicates. The steric bulkiness of the dendrons and the interaction between the layered silicates and ITO glass substrates along with the polyimide capable of interaction-induced orientation brought about the exfoliated morphology, leading to ordered arrangement without applying the poling process. The ordered arrangement behavior was corroborated by UV−visible, VTIR, and EO recovery ratios. Furthermore, the investigation on the dendron/MMT organoclays with different molar ratios also provided the intercalation profiles, revealing that the *d* spacing was influenced by the content of dendrons as well as dendron conformation in the layered confinement. Up to a critical concentration of dendrons in organoclays, the nanocomposites could undergo a conformation change into the ordered arrangement morphology. In addition, the modified organoclay sample with G3 dendrons was also able to exhibit an ordered morphology and subsequently NLO properties without applying the poling process.

Acknowledgment. Financial support from the National Science Council of Taiwan is gratefully acknowledged. This work was also supported in part by the Ministry of Education of Taiwan under the ATU plan.

REFERENCES AND NOTES

(1) Dalton, L. R. *Adv. Polym. Sci.* **2002**, *158*, 1.
(2) Samyn, C.; Verbiest, T.; Persoons, A. *Macromol. Rapid Commun.* **2000**, *21*, 1.
(3) Jeng, R. J.; Chang, C. C.; Chen, C. P.; Chen, C. T.; Su, W. C. *Polymer* **2003**, *44*, 143.
(4) Chang, C. C.; Chen, C. P.; Chou, C. C.; Kuo, W. J.; Jeng, R. J. *J. Macro. Sci., Polym. Rev.* **2005**, *45*, 125.
(5) Chang, H. L.; Lin, H. L.; Wang, Y. C.; Dai, S. H. A.; Su, W. C.; Jeng, R. J. *Polymer* **2007**, *48*, 2046.
(6) Li, Z.; Li, Z.; Di, C.; Zhu, Z.; Li, Q.; Zeng, Q.; Zhang, K.; Liu, Y.; Ye, C.; Qin, J. *Macromolecules* **2006**, *39*, 6951.
(7) Li, Z.; Wu, W.; Yu, G.; Liu, Y.; Ye, C.; Qin, J.; Li, Z. *ACS Appl. Mater. Interfaces* **2009**, *1*, 856.
(8) Wang, Y.; Wang, X.; Guo, Y.; Cui, Z.; Lin, Q.; Yu, W.; Liu, L.; Xu, L.; Zhang, D.; Yang, B. *Langmuir* **2004**, *20*, 8952.
(9) Wang, Y.; Wang, C.; Wang, X.; Guo, Y.; Xie, B; Cui, Z.; Liu, L.; Xu, L.; Zhang, D.; Yang, B. *Chem. Mater.* **2005**, *17*, 1265.
(10) Facchetti, A.; Beverina, L.; Van der Boom, M. E.; Dutta, P.; Evmenenko, G.; Shukla, A. D.; Stern, C. E.; Pagani, G. A.; Marks, T. J. *J. Am. Chem. Soc.* **2006**, *128*, 2142.
(11) Kang, Hu.; Evmenenko, G.; Dutta, P.; Clays, K.; Song, K.; Marks, T. J. *J. Am. Chem. Soc.* **2006**, *128*, 6194.
(12) Ray, S. S.; Okamoto, M. *Prog. Polym. Sci.* **2003**, *28*, 1539.
(13) Lin, J. J.; Cheng, I. J.; Wang, R.; Lee, R. J. *Macromolecules* **2001**, *34*, 8832.
(14) Chou, C. C.; Shieu, F. S.; Lin, J. J. *Macromolecules* **2003**, *36*, 2187.
(15) Lin, J. J.; Chu, C. C.; Chiang, M. L.; Tsai, W. C. *Adv. Mater.* **2006**, *18*, 3248.
(16) Beall, G. W.; Goss, M. *Appl. Clay Sci.* **2004**, *27*, 179.
(17) Lin, J. J.; Chen, I. J.; Chou, C. C. *Macromol. Rapid Commun.* **2003**, *24*, 492.
(18) Osman, M. A.; Ploetze, M.; Skrabal, P. *J. Phys. Chem. B* **2004**, *108*, 2580.
(19) Juang, T. Y.; Cheng, C. T.; Wu, T. M.; Dai, S. A.; Chen, C. P.; Lin, J. J.; Liu, Y. L.; Jeng, R. J. *Nanotechnology* **2007**, *18*, 205606.
(20) Chen, Y. C.; Chang, H. L.; Lee, R. H.; Dai, S. A.; Su, W. C.; Jeng, R. J. *Polym. Adv. Technol.* **2009**, *20*, 493.
(21) Ma, H.; Jen, A. K. Y. *Adv. Mater.* **2001**, *13*, 1201.
(22) Tian, Y.; Chen, C. Y.; Haller, M. A.; Tucker, N. M.; Ka, J. W.; Luo, J.; Huang, S.; Jen, A. K. Y. *Macromolecules* **2007**, *40*, 97.
(23) Cho, M. J.; Choi, D. H.; Sullivan, P. A.; Akelaitis, A. J. P.; Dalton, L. R. *Prog. Polym. Sci.* **2008**, *33*, 1013.
(24) Do, J. Y.; Ju, J. J. *Macromol. Chem. Phys.* **2005**, *206*, 1326.
(25) Li, Z.; Yu, G.; Wu, W.; Liu, Y.; Ye, C.; Qin, J.; Li, Z. *Macromolecules* **2009**, *42*, 3864.
(26) Percec, V.; Ahn, C. H.; Ungar, G.; Yeardley, D. J. P.; Möller, M.; Sheiko, S. S. *Nature* **1998**, *391*, 161.
(27) Ge, Z.; Luo, S.; Liu, S. *J. Polym. Sci., Part A: Polym. Chem.* **2006**, *44*, 1357.
(28) Smith, D. K.; Hirst, A. R.; Love, C. S.; Hardy, J. G; Brignell, S. V; Huang, B. *Prog. Polym. Sci.* **2005**, *30*, 220.
(29) Lo, S. C.; Burn, P. L. *Chem. Rev.* **2007**, *107*, 1097.
(30) Chen, Y. C.; Juang, T. Y.; Dai, S. A.; Wu, T. M.; Lin, J. J.; Jeng, R. J. *Macromol. Rapid Commun.* **2008**, *29*, 587.
(31) Liu, J. G.; Li, Z. X.; Wu, J. T.; Zhou, H. W.; Wang, F. S.; Yang, S. Y. *J. Polym. Sci., Part A: Polym. Chem.* **2002**, *40*, 1583.
(32) Park, J. C.; Park., D. J.; Son, K. C.; Kim, Y. B. *Mol. Cryst. Liq. Cryst.* **2007**, *479*, 191.
(33) Toney, M. F.; Russell, T. P.; Logan, J. A.; Kikuchi, H.; Sands, J. M.; Kumar, S. K. *Nature* **1995**, *374*, 709.
(34) Chen, W.; Feller, M. B.; Shen, Y. R. *Phys. Rev. Lett.* **1989**, *63*, 2665.
(35) Ito, N.; Sakamoto, K.; Arafune, R.; Ushioda, S. *J. Appl. Phys.* **2000**, *88*, 3235.
(36) Liu, Z.; Yu, F.; Zhang, Q.; Zeng, Y.; Wang, Y. *Eur. Polym. J.* **2008**, *44*, 2718.
(37) Okano, K.; Matsuura, N.; Kobayashi, S. *Jpn. J. Appl. Phys.* **1982**, *21*, 109.
(38) Liu, X.; Liu, J.; Jiang, M. *Macromol. Rapid Commun.* **2009**, *30*, 892.
(39) Chen, C. P.; Dai, S. A.; Chang, H. L.; Su, W. C.; Jeng, R. J. *J. Polym. Sci., Part A: Polym. Chem.* **2005**, *43*, 682.

(40) Chen, C. P.; Dai, S. A.; Chang, H. L.; Su, W. C.; Wu, T. M.; Jeng, R. J. *Polymer* **2005**, *46*, 11849.
(41) Tsai, C. C.; Juang, T. Y.; Dai, S. A.; Wu, T. M.; Su, W. C.; Liu, Y. L.; Jeng, R. J. *J. Mater. Chem.* **2006**, *16*, 2056.
(42) Ting, W. H.; Chen, C. C.; Dai, S. A.; Suen, S. Y.; Yang, I. K.; Liu, Y. L.; Chen, F. M. C.; Jeng, R. J. *J. Mater. Chem.* **2009**, *19*, 4819.
(43) Teng, C. C.; Man, H. T. *Appl. Phys. Lett.* **1990**, *56*, 1734.
(44) Acosta, E. J.; Deng, Y.; White, G. N.; Dixon, J. B.; McInnes, K. J.; Senseman, S. A.; Frantzen, A. S.; Simanek, E. E. *Chem. Mater.* **2003**, *15*, 2903.
(45) Beckers, E. H. A.; Meskers, S. C. J.; Schenning, A. P. H.; Chen, Z.; Wŕthner, F.; Marsal, P.; Beljonne, D.; Jĕrŏme, C.; Janssen, E. A. J. *J. Am. Chem. Soc.* **2006**, *128*, 649.
(46) Du, X.; Wang, Y. *J. Phys. Chem. B.* **2007**, *111*, 2347.
(47) Marras, S. I.; Tsimpliaraki, A.; Zuburtikudis, I.; Panayiotou, C. *J. Colloid Inter. Sci.* **2007**, *315*, 520.
(48) Alexandre, M.; Dubois, P. *Mater. Sci. Eng. Res.* **2000**, *28*, 1.
(49) Wang, B. B.; Zhang, X.; Jia, X. R.; Li, Z. C.; Ji, Y.; Yang, L.; Wei, Y. *J. Am. Chem. Soc.* **2004**, *126*, 15180.

AM900499S